Available online at www.sciencedirect.com
SCIENCE DIRECT®
Journal of Hydrology 298 (2004) 136–154
Journal of Hydrology
www.elsevier.com/locate/jhydrol

# Formulation of a hybrid calibration approach for a physically based distributed model with NEXRAD data input

Mauro Di Luzio[a,*], Jeffrey G. Arnold[b,1]

[a]*Blackland Research Center, Texas Agricultural Experiment Station, Texas A&M University System, 720 E. Blackland Rd, Temple, TX 76502, USA*
[b]*Grassland Research Laboratory, United States Department of Agriculture-Agricultural Research Service, 808 E. Blackland Rd, Temple, TX 76502, USA*

Received 17 June 2003; revised 12 January 2004; accepted 29 March 2004

**Abstract**

This paper describes the background, formulation and results of an hourly input–output calibration approach proposed for the Soil and Water Assessment Tool (SWAT) watershed model, presented for 24 representative storm events occurring during the period between 1994 and 2000 in the Blue River watershed (1233 $km^2$ located in Oklahoma).

This effort is the first follow up to the participation in the National Weather Service-Distributed Modeling Intercomparison Project (DMIP), an opportunity to apply, for the first time within the SWAT modeling framework, routines for hourly stream flow prediction based on gridded precipitation (NEXRAD) data input. Previous SWAT model simulations, uncalibrated and with moderate manual calibration (only the water balance over the calibration period), were provided for the entire set of watersheds and associated outlets for the comparison designed in the DMIP project.

The extended goal of this follow up was to verify the model efficiency in simulating hourly hydrographs calibrating each storm event using the formulated approach. This included a combination of a manual and an automatic calibration approach (Shuffled Complex Evolution Method) and the use of input parameter values allowed to vary only within their physical extent.

While the model provided reasonable water budget results with minimal calibration, event simulations with the revised calibration were significantly improved. The combination of NEXRAD precipitation data input, the soil water balance and runoff equations, along with the calibration strategy described in the paper, appear to adequately describe the storm events.

The presented application and the formulated calibration method are initial steps toward the improvement of the simulation on an hourly basis of the SWAT model loading variables associated with the storm flow, such as sediment and pollutants, and the success of Total Maximum Daily Load (TMDL) projects.


*Keywords:* Simulation; Pollution; GIS; Non-point source

## 1. Introduction

During major storms, flooding and the life-threatening flood flows and property losses are certainly the most stringent and evident

* Corresponding author. Tel.: +1-254-774-6138; fax: +1-254-774-6001.
*E-mail addresses:* diluzio@brc.tamus.edu (M. Di Luzio), jgarnold@spa.ars.usda.gov (J.G. Arnold).
[1] Tel.: +1-254-770-6502; fax: +1-254-770-6561.

0022-1694/$ - see front matter © 2004 Elsevier B.V. All rights reserved.
doi:10.1016/j.jhydrol.2004.03.034

consequences. Concurrently, and more silently, runoff from farmland, city streets, construction sites, and sub-urban lawns, roofs and driveways enters waterways, often carrying high quantities of harmful substances such as sediments, excess nutrients, pathogens and toxic substances. This component of the water runoff, widely known as Non-point Source Pollution (NPS), is contributing worldwide to stream water degradation. In many countries, environmental agencies are making efforts to assess and suggest actions to lessen the NPS impact. In the United States, NPS is recognized as the leading cause of the water quality impairment and the Environmental Protection Agency (USEPA), by the Total Maximum Daily Load (TMDL) program, is requiring states to develop lists of critical water bodies on a watershed-by-watershed basis and prepare detailed plans for reducing pollutant loading from stormwater and agricultural land. Within these programs, the required evaluation of alternative management, land use, and conservation practices is essentially accomplished using NPS models.

Basically, NPS models are extended hydrologic models, including additional modules for the evaluation of erosion and sediment delivery, as well as the release, leaching and loading of pollutants from the land. At the watershed scale, these models are paralleling the evolution of hydrologic models for flow simulation. Increasing computer and Geographic Information System (GIS) capability and spatial data set availability are providing continuously enhanced representations of large inhomogeneities in the hydrologic properties of the watersheds, thereby supporting the development of distributed models. Distributed NPS models have the ability to provide simulation time series at stream reaches and sections, as well as locate critical areas, moisture and pollutant levels, within the entire simulated watershed. Continuous time vs. event based NPS models have the capability to simulate crop growth, management and conservation cropping systems, all acting in different degrees and during different times of the hydrologic year. In addition, continuous NPS models provide simulation output and status variables, regardless of storm size. In fact, while large events generally produce large amounts of runoff, erosion, and delivery of pollutants, smaller events control many of the antecedent parameters that modulate sediment yield and pollutant remobilization from large events. Continuous simulations of hydrological processes that occur between storms are also important when low flow conditions may provide potential threatening conditions for aquatic life including the situation when oxygen concentration drops to the depletion level.

The more recent availability of high spatial and temporal resolution precipitation estimates from modern radar networks appears to provide further potential for advancements of distributed NPS models. In particular, the simulation enhancement of the storm water dynamics and associated pollutant phases appear to be the most promising direction of development. Traditional NPS model applications, requiring the capability to evaluate and compare developing alternative management practices over long-term periods and on large ungauged stream watersheds, have been relying either on generated rainfall data or on daily rainfall records. This is also justified when considering that NPS models are also required to be tools with enough simplicity to shield users from the extreme complexity of the hydrologic processes and with minimal amount of user input data, while providing alternative agriculture management practice scenario comparisons.

The Soil and Water Assessment Tool (SWAT) (Arnold et al., 1998) is a semi-distributed, continuous NPS model developed to assist water resource managers in assessing the impact of management and climate on water supplies and NPS in watersheds and large river basins. The model is physically based, computationally efficient, and capable of simulating a high level of spatial details by allowing the watershed to be divided into a large number of sub-watersheds. Major model components include: hydrology, erosion/sedimentation, plant growth, nutrients, pesticides, land management, stream routing, and pond/reservoir routing. SWAT is designed to predict the impact of management on water, sediment, and agricultural chemical yields, operating on a daily time step. The model has been validated for several watersheds (Arnold et al., 1999). The model was developed in the early 1990s and represents over thirty years of model improvement within the US Department of Agriculture's Agriculture Research Service (USDA-ARS). The model is provided with an operational interface in ArcView GIS, AVSWAT (Di Luzio et al., 2004), for the definition of the watershed

hydrologic features; storage, organization, manipulation of the related spatial and tabular data; and analyses of management scenarios.

We proposed the SWAT model system for participation in the Distributed Model Intercomparison Project (DMIP) (Smith et al., 2004). Our motivation was to take an initial step toward understanding the issues pertaining to the use of NEXRAD Stage III (Fulton et al., 1998) gridded precipitation data with a 1-h temporal and 4-km spatial resolution within the SWAT model. Previous applications of the model with input at shorter temporal resolution than 1 day used break point raingage data records on a small watershed with daily based assessment of the simulation efficiency (King et al., 1999).

Our long-range objectives are the evaluation of potential and operational advantages of using the NEXRAD data sets, as well as to determine pitfalls and consequent refinements of the hydrologic component of the model, while preserving the requirements of the NPS models described above. The DMIP working procedure, organized by NOAA/National Weather Service, has the potential to reduce the time of SWAT model enhancement by exposing and comparing it to more developed and advanced storm modeling efforts.

For DMIP, the SWAT model was applied to the entire spectrum of the established watersheds and simulation periods (Reed et al., 2004). Given the lack of implemented automatic calibration routines in SWAT, simulations use the default values provided by AVSWAT and a minimal manual calibration focused on the overall water balance. A further automatic calibration effort continues for the Blue River watershed case study (Smith et al., 2004) and the 24 representative events.

In this paper we provide the analyses of the simulation results of a formulated combination of a manual and an automatic calibration approach. Initially the paper summarizes the model and GIS methods implemented as useful quick references and as a baseline for the DMIP models intercomparison.

Specifically, the paper is composed of the following sections: (1) the SWAT model structure, the rainfall-runoff, and the overland and channel routing methods; (2) the input GIS data and procedures developed to ingest the NEXRAD-based products and provide the model rainfall record input; (3) the description of the initial and the minimal calibration methods and results; (4) results and comparison of the developed calibration for the selected events, ultimately the focus of this paper.

## 2. Model formulation and GIS support

In SWAT, a watershed is divided into multiple sub-watersheds, which are then further subdivided into unique soil/land use categories called hydrologic response units (HRUs). The water balance of each HRU in SWAT is represented by four storage volumes: snow, soil profile (0–2 m), shallow aquifer (typically 2–20 m), and deep aquifer (>20 m). Flow generation, sediment yield, and non-point-source loadings from each HRU in a sub-watershed are summed, and the resulting loads are routed through channels, ponds, and/or reservoirs to the watershed outlet.

The soil profile is subdivided into multiple layers that support soil water processes including infiltration, evaporation, plant uptake, lateral flow, and percolation to lower layers. The soil percolation component of SWAT uses a storage routing technique to predict flow through each soil layer in the root zone. Downward flow occurs when field capacity of a soil layer is exceeded and the layer below is not saturated. Percolation from the bottom of the soil profile recharges the shallow aquifer. If the temperature in a particular layer is 0 °C or below, no percolation is allowed from that layer. Lateral sub-surface flow in the soil profile is calculated simultaneously with percolation. Groundwater flow contribution to total stream flow is simulated by routing a shallow aquifer storage component to the stream (Arnold et al., 1993).

Surface runoff from daily rainfall is estimated using: (1) the Green and Ampt infiltration equation or (2) a modified SCS curve number method, which estimates the amount of runoff based on local land use, soil type, and antecedent moisture condition. A provision for estimating runoff from frozen soil is also included. Snow melts on days when the maximum temperature exceeds 0 °C. Melted snow is treated the same as rainfall for estimating runoff and percolation. Channel routing is simulated using the Muskingum method.

The model computes evaporation from soils and plants separately. Potential evapotranspiration is

modeled with the Penman–Monteith, Priestley–Taylor, or Hargreaves method. Potential soil water evaporation is estimated as a function of potential ET and leaf area index (area of plant leaves relative to the soil surface area). Actual soil evaporation is estimated by using exponential functions of soil depth and water content. Plant water evaporation is simulated as a linear function of potential ET, leaf area index and root depth and can be limited by soil water content. More detailed descriptions of the model can be found in Arnold et al. (1998).

Surface runoff from sub-daily (i.e. hourly) rainfall, along with the associated upland and channel routing formulation, are described below.

### 2.1. Infiltration and rainfall excess

The Green and Ampt (1911) and Mein and Larson (1973) excess rainfall method was incorporated into SWAT (King et al., 1999) to provide an alternative option for determining surface runoff. The Green-Ampt Mein-Larson infiltration rate is defined as

$$f_{\mathrm{inf},t} = K_{\mathrm{e}}\left(1 + \frac{\Psi_{\mathrm{wf}}\Delta\theta_{\mathrm{v}}}{F_{\mathrm{inf},t}}\right) \tag{1}$$

where $f_{\mathrm{inf}}$ is the infiltration rate at time $t$ (mm/h); $K_{\mathrm{e}}$, the effective hydraulic conductivity (mm/h); $\Psi_{\mathrm{wf}}$, the wetting front matric potential (mm); $\Delta\theta_{\mathrm{v}}$, the change in volumetric moisture content across the wetting front (mm/mm); $F_{\mathrm{inf}}$ is the cumulative infiltration at time $t$ (mm).

When the rainfall intensity is less than the infiltration rate, all the rainfall will infiltrate during the time period and the cumulative infiltration for that time period is calculated

$$F_{\mathrm{inf},t} = F_{\mathrm{inf},t-1} + R_{\Delta t} \tag{2}$$

where $F_{\mathrm{inf},t}$ is the cumulative infiltration for a given time step (mm); $F_{\mathrm{inf},t-1}$, the cumulative infiltration for the previous time step (mm); $R_{\Delta t}$ is the amount of rain falling during the time step (mm).

The infiltration rate defined by Eq. (1) is a function of the infiltrated volume, which in turn is a function of the infiltration rates in previous time steps. To avoid numerical errors over long time steps, $f_{\mathrm{inf}}$ is replaced by $\mathrm{d}F_{\mathrm{inf}}/\mathrm{d}t$ in Eq. (1) and integrated to obtain

$$F_{\mathrm{inf},t} = F_{\mathrm{inf},t-1} + K_{\mathrm{e}}\Delta t + \Psi_{\mathrm{wf}}\Delta\theta_{\mathrm{v}} \times \ln\left[\frac{F_{\mathrm{inf},t} + \Psi_{\mathrm{wf}}\Delta\theta_{\mathrm{v}}}{F_{\mathrm{inf},t-1} + \Psi_{\mathrm{wf}}\Delta\theta_{\mathrm{v}}}\right] \tag{3}$$

Eq. (3) is solved iteratively for $F_{\mathrm{inf},t}$, the cumulative infiltration at the end of the time step. A successive substitution technique is used.

The Green-Ampt effective hydraulic conductivity parameter, $K_{\mathrm{e}}$, is approximately equivalent to one-half the saturated hydraulic conductivity of the soil, $K_{\mathrm{sat}}$ (Bouwer, 1966). Nearing et al. (1996) developed an equation to calculate the effective hydraulic conductivity as a function of saturated hydraulic conductivity and curve number. This equation incorporates land cover impacts into the calculated effective hydraulic conductivity. The equation for effective hydraulic conductivity is

$$K_{\mathrm{e}} = \frac{56.82K_{\mathrm{sat}}^{0.286}}{1 + 0.051\exp(0.062\mathrm{CN})} - 2 \tag{4}$$

where $K_{\mathrm{e}}$ is the effective hydraulic conductivity (mm/h); $K_{\mathrm{sat}}$, the saturated hydraulic conductivity (mm/h); CN is the curve number.

For each time step, SWAT calculates the amount of water entering the soil. The water that does not infiltrate into the soil becomes surface runoff.

### 2.2. Wetting front redistribution

Wetting front redistribution is calculated for each soil layer in the profile. Water is allowed to percolate if the water content exceeds the field capacity water content for that layer. When the soil layer is frozen, no water flow out of the layer is calculated. The volume of water available for percolation in the soil layer is calculated

$$\mathrm{SW}_{\mathrm{ly,excess}} = \mathrm{SW}_{\mathrm{ly}} - \mathrm{FC}_{\mathrm{ly}} \qquad \text{if } \mathrm{SW}_{\mathrm{ly}} > \mathrm{FC}_{\mathrm{ly}} \tag{5}$$

$$\mathrm{SW}_{\mathrm{ly,excess}} = 0 \qquad \text{if } \mathrm{SW}_{ly} \le \mathrm{FC}_{\mathrm{ly}} \tag{6}$$

where $\mathrm{SW}_{\mathrm{ly,excess}}$ is the drainable volume of water in the soil layer on a given day; $\mathrm{SW}_{\mathrm{ly}}$, the water content of the soil layer on a given day; $\mathrm{FC}_{\mathrm{ly}}$ is the water content of the soil layer at field capacity, all in mm.

The amount of water that moves from one layer to the underlying layer is calculated using storage

routing methodology. The equation used to calculate the amount of water that percolates to the next layer is

$$w_{\mathrm{perc,ly}} = \mathrm{SW}_{\mathrm{ly,excess}}\left(1 - \exp\left[\frac{-\Delta t}{\mathrm{TT}_{\mathrm{perc}}}\right]\right) \tag{7}$$

where $w_{\mathrm{perc,ly}}$ is the amount of water percolating to the underlying soil layer on a given day (mm); $\mathrm{SW}_{\mathrm{ly,excess}}$, the drainable volume of water in the soil layer on a given day (mm); $\Delta t$, the length of the time step (h); $\mathrm{TT}_{\mathrm{perc}}$ is the travel time for percolation (h).

The travel time for percolation is unique for each layer is calculated as follow

$$\mathrm{TT}_{\mathrm{perc}} = \frac{\mathrm{SAT}_{\mathrm{ly}} - \mathrm{FC}_{\mathrm{ly}}}{K_{\mathrm{sat}}} \tag{8}$$

where $\mathrm{TT}_{\mathrm{perc}}$ is the travel time for percolation (h); $\mathrm{SAT}_{\mathrm{ly}}$, the amount of water in the soil layer when completely saturated (mm); $\mathrm{FC}_{\mathrm{ly}}$, the water content of the soil layer at field capacity (mm); $K_{\mathrm{sat}}$ is the saturated hydraulic conductivity for the layer (mm/h). Water that percolates out of the lowest soil layer enters the vadose zone.

### 2.3. Direct runoff

Direct runoff, or runoff before it reaches the stream, is calculated using hourly rainfall excess and the SCS triangular unit hydrograph (Pilgrim and Cordery, 1992) The time to peak of the hydrograph is

$$T_{\mathrm{p}} = 0.5D + 0.6t_{\mathrm{c}} \tag{9}$$

where $D$ is the rainfall excess duration (h) and $t_{\mathrm{c}}$ is the time of concentration (h), the volume of runoff under the hydrograph is $\frac{1}{2}q_{\mathrm{p}}T_{\mathrm{b}}$, where $T_{\mathrm{b}}$ is the base length of the hydrograph and is assumed equal to $2.67T_{\mathrm{p}}$, based on the study of many unit hydrographs. Equating this volume to $Q$, the volume estimated from the rainfall (mm), and then combining the above relations, rearranging and adjusting for units, the peak discharge $q_{\mathrm{p}}$ ($\mathrm{m}^3/\mathrm{s}$) is given by

$$q_{\mathrm{p}} = \frac{0.208AQ}{0.5D + 0.6t_{\mathrm{c}}} \tag{10}$$

where $A$ is the area of the drainage basin ($\mathrm{km}^2$).

### 2.4. Channel routing

Manning's equation for uniform flow in a channel is used to calculate the rate and velocity of flow in a reach segment for a given time step

$$q_{\mathrm{ch}} = \frac{A_{\mathrm{ch}}R_{\mathrm{ch}}^{2/3}\mathrm{slp}_{\mathrm{ch}}^{1/2}}{n} \tag{11}$$

$$v_{\mathrm{c}} = \frac{R_{\mathrm{ch}}^{2/3}\mathrm{slp}_{\mathrm{ch}}^{1/2}}{n} \tag{12}$$

where $q_{\mathrm{ch}}$ is the rate of flow in the channel ($\mathrm{m}^3/\mathrm{s}$); $A_{\mathrm{ch}}$, the cross-sectional area of flow in the channel ($\mathrm{m}^2$); $R_{\mathrm{ch}}$, the hydraulic radius for a given depth of flow (m); $\mathrm{slp}_{\mathrm{ch}}$, the slope along the channel length (m/m); $n$, Manning's 'n' coefficient for the channel; $v_{\mathrm{c}}$ is the flow velocity (m/s).

Depth of flow is calculated in the channel assuming a trapezoidal channel

$$\mathrm{depth} = \sqrt{\frac{A_{\mathrm{ch}}}{z_{\mathrm{ch}}} + \left(\frac{W_{\mathrm{btm}}}{2z_{\mathrm{ch}}}\right)^2} - \frac{W_{\mathrm{btm}}}{2z_{\mathrm{ch}}} \tag{13}$$

where *depth* is the depth of flow (m); $A_{\mathrm{ch}}$, the cross-sectional area of flow in the channel for a given depth of water ($\mathrm{m}^2$), $W_{\mathrm{btm}}$, the bottom width of the channel (m); $z_{\mathrm{ch}}$ is the inverse of the channel side slope. Eq. (13) is valid only when all water is contained in the channel. If the volume of water in the reach segment has filled the channel and is in the flood plain, the depth is calculated

$$\mathrm{depth} = \mathrm{depth}_{\mathrm{bnkfull}} + \sqrt{\frac{(A_{\mathrm{ch}} - A_{\mathrm{ch,bnkfull}})}{z_{\mathrm{fld}}} + \left(\frac{W_{\mathrm{btm,fld}}}{2z_{\mathrm{fld}}}\right)^2} - \frac{W_{\mathrm{btm,fld}}}{2z_{\mathrm{fld}}} \tag{14}$$

where *depth* is the depth of flow (m); $\mathrm{depth}_{\mathrm{bnkfull}}$, the depth of water in the channel when filled to the top of the bank (m); $A_{\mathrm{ch}}$, the cross-sectional area of flow in the channel for a given depth of water ($\mathrm{m}^2$); $A_{\mathrm{ch,bnkfull}}$, the cross-sectional area of flow in the channel when filled to the top of the bank ($\mathrm{m}^2$); $W_{\mathrm{btm,fld}}$, the bottom width of the flood plain (m); $z_{\mathrm{fld}}$ is the inverse of the flood plain side slope.

The classic Muskingum routing method models the storage volume in a channel as a combination of

wedge and prism storage. When a flood wave advances into a reach segment, inflow exceeds outflow and a wedge of storage is produced. As the flood wave recedes, outflow exceeds inflow in the reach segment and a negative wedge is produced. In addition to the wedge storage, the reach segment contains a prism of storage formed by a volume of constant cross-section along the reach length.

The definition for storage volume can be incorporated into the continuity equation and simplified to

$$q_{out,2} = C_1 q_{in,2} + C_2 q_{in,1} + C_3 q_{out,1} \quad (15)$$

where $q_{in,1}$ is the inflow rate at the beginning of the time step ($m^3/s$); $q_{in,2}$, the inflow rate at the end of the time step ($m^3/s$); $q_{out,1}$, the outflow rate at the beginning of the time step ($m^3/s$); $q_{out,2}$ is the outflow rate at the end of the time step ($m^3/s$), and

$$C_1 = \frac{\Delta t - 2KX}{2K(1-X) + \Delta t} \quad (16)$$

$$C_2 = \frac{\Delta t + 2KX}{2K(1-X) + \Delta t} \quad (17)$$

$$C_3 = \frac{2K(1-X) - \Delta t}{2K(1-X) + \Delta t} \quad (18)$$

where $C_1 + C_2 + C_3 = 1$. To express all values in units of volume, both sides of Eq. (15) are multiplied by the time step

$$V_{out,2} = C_1 V_{in,2} + C_2 V_{in,1} + C_3 V_{out,1} \quad (19)$$

To maintain numerical stability and avoid the computation of negative outflows, the following condition must be met:

$$2KX < \Delta t < 2K(1-X) \quad (20)$$

The value for the weighting factor, $X$, is input by the user. The value for the storage time constant was modified as

$$K = \mathrm{coef}_1 K_{bnkfull} + \mathrm{coef}_2 K_{0.1bnkfull} \quad (21)$$

where $K$ is the storage time constant for the reach segment (s); $\mathrm{coef}_1$ and $\mathrm{coef}_2$, the weighting coefficients input by the user; $K_{bnkfull}$, the storage time constant calculated for the reach segment with bankfull flows (s); $K_{0.1bnkfull}$ is the storage time constant calculated for the reach segment with one-tenth of the bankfull flows (s). To calculate $K_{bnkfull}$ and $K_{0.1bnkfull}$, an equation developed by Cunge (1969) is used

$$K = \frac{1000 L_{ch}}{c_k} \quad (22)$$

where $K$ is the storage time constant (s); $L_{ch}$, the channel length (km); $c_k$ is the celerity corresponding to the flow for a specified depth (m/s). Celerity is the velocity with which a variation in flow rate travels along the channel. It is defined by differentiating Eq. (11) with respect to the cross-sectional area as shown in Eq. (23)

$$c_k = \frac{5}{3}\left(\frac{R_{ch}^{2/3} \mathrm{slp}_{ch}^{1/2}}{n}\right) = \frac{5}{3} v_c \quad (23)$$

where $c_k$ is the celerity (m/s); $R_{ch}$, the hydraulic radius for a given depth of flow (m); $\mathrm{slp}_{ch}$, the slope along the channel length (m/m); $n$, Manning's 'n' coefficient for the channel; $v_c$ is the flow velocity (m/s).

### 2.5. GIS support

A customized extension for the ArcView GIS 3.x software (ESRI, 1996a), AVSWAT (ArcView SWAT) (Di Luzio et al., 2004), was utilized to prepare the input for the applied version of the model (version 2000). AVSWAT provides a full range of user-friendly and interactive input/output manipulation tools designed to help the user perform numerous tasks required in efficiently using the SWAT model. In this project, fundamental AVSWAT components were used for the following:

(a) Segmentation and dimensioning of the watershed in composing sub-watersheds and associated stream channels using digital terrain data provided by a Digital Elevation Model (DEM). The channel active head and the associated synthetic stream network were defined using a uniform threshold value on the DEM-derived cumulated drainage area. Outlets of the respective sub-watersheds located, by default, on each junction of the defined stream network. Additional outlets located at the stream sections at which model outputs were requested for this project (i.e. interior points).

(b) Parameterization of each sub-watershed by the composing HRUs. Each HRU defined as a unique combination of soil and land use/land cover elementary classes within the sub-watershed. The distribution

of the HRUs within each modeling sub-watershed was determined using an AVSWAT built-in tool. A further step provided options for the users to choose either a predominant HRU for each sub-watershed or controlling the total number of HRUs units based on two specified thresholds of land uses and soils percentage. Specifically, within the extent of each sub-watershed, land use classes covering a percentage of area less than an input threshold value are ignored while the area of retained classes are proportionally adjusted to fill the removed areas. Similarly, but within the extent of each land use class in each sub-watershed, soil classes covering a percentage of area less than an input threshold value are ignored. We used a typical value (30%) for the land use/land cover threshold while, since soil properties are important for simulation of the water infiltration, soil percentage threshold of 0% allowed retention of the entire spectrum of soils within each sub-watershed/land use area.

(c) Calculation of the mean areal precipitation for each sub-watershed. An additional procedure within AVSWAT was built using AVENUE (ESRI, 1996b) to extract data files from compressed file archives and process the NEXRAD gridded values, each grid covering a $4 \times 4\ km^2$ area, and referenced by the HRAP (Hydrologic Rainfall Analysis Project) (Reed and Maidment, 1999) coordinate system. For each sub-watershed, the set of HRAP grid areas intersecting it were identified, and the respective mean areal precipitation for each hourly time step calculated as an area-weighted average of the identified gridded precipitation values.

## 3. Model inputs and calibration

### 3.1. Model inputs

The SWAT version 2000 (Arnold et al., 2002) was set up using AVSWAT and applied to the entire set of case study watersheds along with the associated outlets and the interior points proposed for the DMIP project. The main set of simulated watershed systems includes: (1) Blue River at Blue, OK; (2) Elk River at Tiff City, MO; (3) Baron Fork at Eldon, OK; (4) Illinois River at Tahlequah, OK. Simulation set (3) also included Peacheater Creek at Christie, OK, sub-watershed; simulation set (4) included Flint Creek at Kansas, OK, Illinois River at Watts, OK, and Illinois River at Savoy, OK, sub-watersheds, listed by Smith et al. (2004) along with their description. Besides the NEXRAD data provided for this project, the model was set up using AVSWAT and the following data sets:

(a) Three arc-second (spatial resolution around 90 m), 1:250,000-scale, USGS DEM (USGS, 1993).
(b) National Hydrography Dataset (NHD) (USGS and USEPA, 2000), Cataloging Unit 11140102, used within AVSWAT as hydrography layer to support the stream definition using a DEM 'burning' method (Di Luzio et al., 2004).
(c) USGS (United States Geological Survey), National Land Cover Data (Vogelmann et al., 2001), based primarily on 1992 vintage Landsat 5 Thematic Mapper, spatial resolution 30 m.
(d) STATSGO (State Soil Geographic) Database layer (USDA-NRCS, 1992), 1:250,000-scale. soil map in shape-polygon format. Soil hydraulic parameters were extracted from a database included in AVSWAT. This data base derives from a linkage of STATSGO map units to the respective soil records elaborated using the MUUF (Map Unit User Files) method (Baumer et al., 1994).

All these data sets are alternative to those provided for DMIP, since only the usage of NEXRAD rainfall series was specifically required.

Table 1 shows the number of sub-watersheds and HRUs used to simulate the case study basins.

### 3.2. Calibration

The overall goal of the model calibration was to establish an objective initial strategy for parameter estimation that provides consistent performance by eliminating the kinds of subjective human judgments involved in a traditional manual approach Moreover, in our gradual assimilation of the issues pertaining the use of the NEXRAD data, there was a need to verify, for the first time, if the current SWAT model framework along with the associate sub-daily routines were able to adequately simulate, within a physically

based space of the input parameters, fundamental portions of the hydrographs (storm flow). This verification is a prerequisite for future improvement of the assessment of pollutant loadings.

Extensive research has been devoted to the attempt to identify optimal criteria (Sooroshian and Dracop, 1980; Kuczera, 1983) and optimization algorithms (Duan et al., 1992; Sooroshian et al., 1993). Most of the automatic calibration routines have been based on a single mathematical criterion or objective measure. More recently automatic routines based on multi-objective formulation of the calibration problem have been introduced in hydrologic modeling (Lindström, 1997; Gupta et al., 1998; Yapo et al., 1998; Boyle et al., 2000) in order to overcome weaknesses of the single objective approach.

Another kind of automatic calibration approach involves the knowledge-based expert systems in order to tailor methods against specific model applications (Madsen et al., 2002). With these approaches, the calibration procedure reproduces the course of a trial-and-error calibration of an experienced hydrologist focusing on the numerical optimization of different process descriptions. Similarly, a variety of hybrid approaches combine the strengths of manual and automatic calibration strategies (Gupta et al., 1998; Boyle et al., 2000) resulting in efficient, yet acceptable estimates for the parameters of a conceptual hydrologic model.

In general, the most advanced of these approaches allow the user to intervene at different levels and different stages in the calibration process, putting emphasis on different response modes of the hydrograph. It appears, besides the problem of non-uniqueness in model calibration associated with the choice of the performance measures, that calibration approaches based on user-specified calibration priorities in combination with generic search routines compared satisfactorily with approaches requiring various degrees of user intervention during the entire calibration process (Madsen, 2002).

In this perspective our priorities in this study were: (1) anchor the simulation around a satisfactory water budget (manual calibration); (2) calibrate the SWAT model hydrograph during various single events (automatic calibration).

The two approaches involve the use of progressively more sophisticated procedures for refining the parameter estimates by the use of input–output time series data collected for the study watersheds. In a different way the methods employed in both approaches involve: (a) the evaluation of the 'distance' between the model outputs and the corresponding observed data; and (b) adjustment

Table 1
Summary of basins, simulation settings and basic calibration results for the SWAT model applications in DMIP

| Basin | Number of sub-watersheds | Number of HRUs | Average yearly flow (mm) | | | |
|---|---|---|---|---|---|---|
| | | | Runoff type | Observed | Simulated no calibration | Simulated minimal calibration |
| Blue River at Blue, OK | 55 | 177 | Total | 269 | 395 | 249 |
| | | | Surface | 140 | 131 | 137 |
| | | | Baseflow | 129 | 261 | 112 |
| Elk River at Tiff City, MO | 118 | 346 | Total | 432 | 630 | 442 |
| | | | Surface | 160 | 368 | 177 |
| | | | Baseflow | 272 | 262 | 266 |
| Baron Fork at Eldon, OK | 43 | 138 | Total | 511 | 594 | 510 |
| | | | Surface | 205 | 279 | 173 |
| | | | Baseflow | 306 | 315 | 338 |
| Illinois River at Talequa, OK | 124 | 397 | Total | 338 | 551 | 371 |
| | | | Surface | 115 | 267 | 112 |
| | | | Baseflow | 223 | 287 | 259 |

of the values of the parameters to reduce the 'distance'. In addition, although input parameters to the model are physically based there is often considerable uncertainty associated with the values due to spatial variability, measurement methods, etc. Common to the methods employed in the two approaches is that input parameters were allowed to vary only within a given realistic uncertainty range to calibrate the components of the streamflow.

*3.2.1. Manual calibration*

The approach used in this calibration phase involved the evaluation of the 'distance' after a number of semi-intuitive trial and error processes used to perform the parameter adjustment. In our studies the goal was to adjust the simulation of the average annual contributions to the watershed runoff budget based on the available stream discharge observations. These contributions were determined using an automatic baseflow separation algorithm (Arnold et al., 1995). Surface and baseflow runoff were considered the contributions to the overall streamflow.

Key input parameters have been selected based on our experience and an understanding of the model structure. Namely, the following model parameters

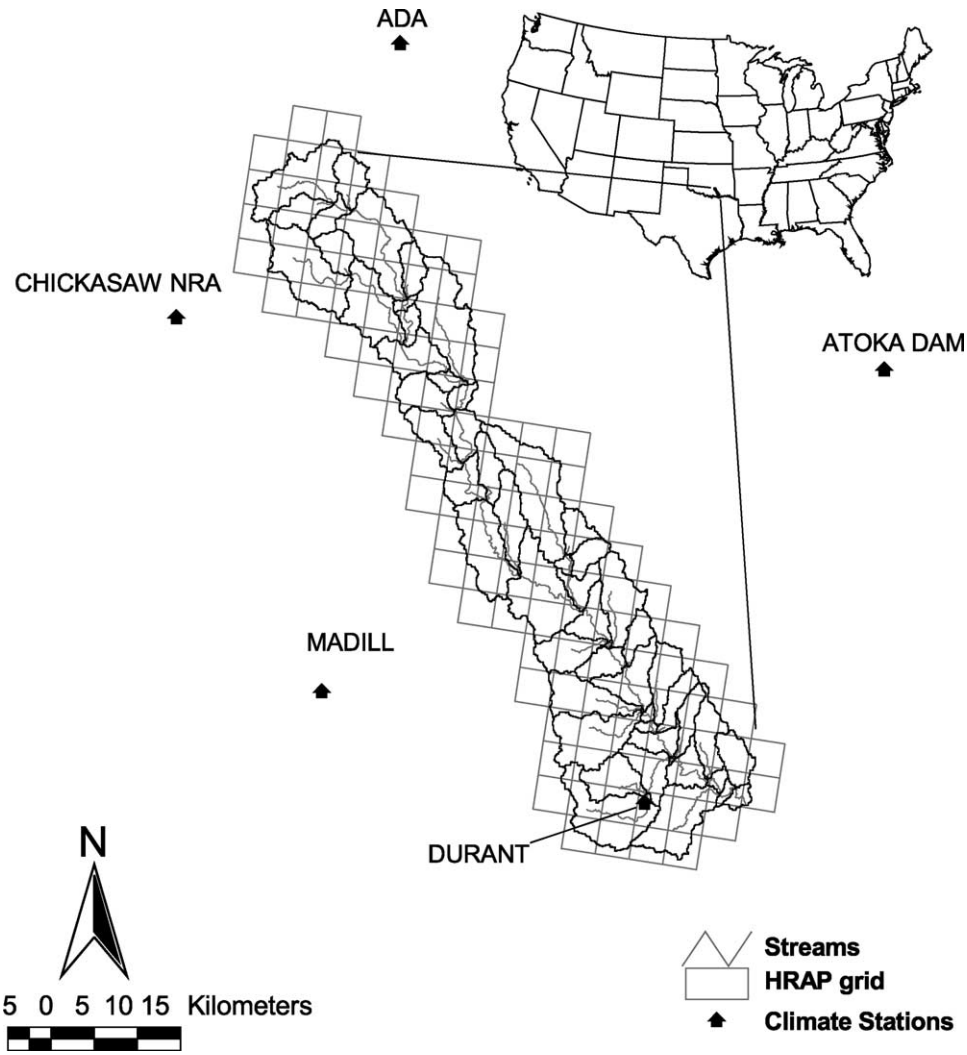


Fig. 1. Blue River basin sub-watershed delineation, HRAP grid, with climate stations indicated.

were adjusted: soil saturated hydraulic conductivity (SOL_K), soil evaporation compensation factor (ESCO), total number of heat units or growing degree days needed to bring plant to maturity (PHU), and potential or maximum crack volume of the soil profile (SOL_CRK). The values of these parameters have been manually, iteratively and uniformly adjusted by a constant factor over all the HRUs until the overall simulated water balance and discharge contributions were close to the observed values and a consequent heuristic optimum was reached.

### 3.2.2. Automatic calibration

Our approach involved the pre-selection of key input parameters and the definition of the respective region of the space considered to contain feasible values for the parameters. This selection is not specific to a particular watershed and it has been based on our experience and an understanding of the model structure. As mentioned above, bounds of the parameter values have been established based on their physical scope. In this way we warrant that calibrated simulations are hydrologically realistic and not the result of pure curve-fitting.

A classical approach was followed to: (a) evaluate, using a mathematical criterion, the differences between the simulated and the observed hydrographs, and (b) adjust the parameters using an optimization algorithm. We also used a single objective measure of comparison, the sum of the squares of the residuals (SSQ), in Eq. (24), since this study represents an initial process of investigation of the issues implicated

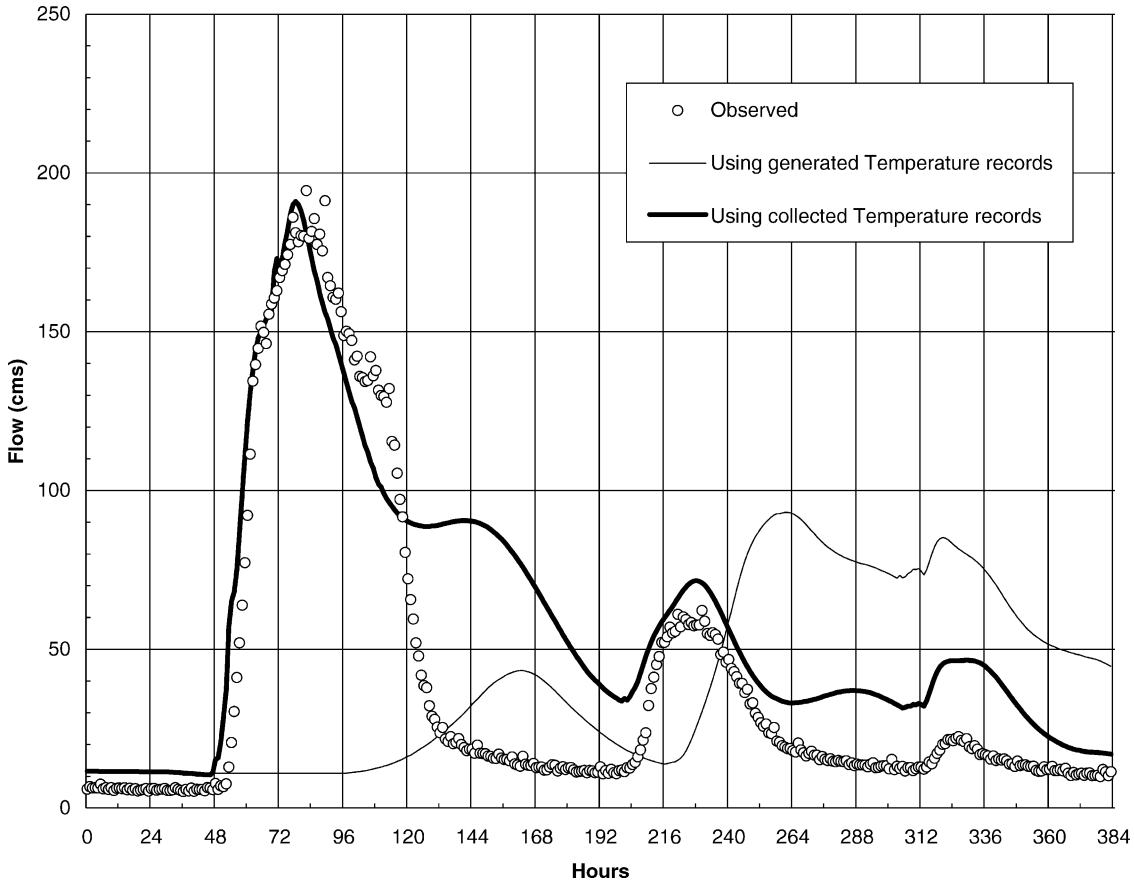


Fig. 2. Simulation of a storm event (February 20–26, 1997), Blue River basin. Solid line shows results using collected temperature records; dashed line shows results using generated temperature records.

with the model calibration on an hourly basis

$$\mathrm{SSQ} = \sum_{i=1,n} [x_{i,\mathrm{measured}} - x_{i,\mathrm{simulated}}]^2 \quad (24)$$

where $n$ is the number of pairs of measured ($x_{\mathrm{measured}}$) and simulated ($x_{\mathrm{simulated}}$) variables.

Among the several optimization algorithms available, we have chosen the Shuffled Complex Evolution Method (SCE) (Duan, 1991; Sorooshian et al., 1993), recognized in the literature to be both robust and efficient. In brief, the SCE algorithm provides a searching strategy over the whole input parameter spaces to find the global optimum. The searching strategy combines a systematic evolution of points in the direction of global improvement, competitive evolution, and the concept of complex shuffling. As it searches over the whole parameter space, the algorithm finds the global optimum using an approach that treats the global search as a process of natural evolution (Duan et al., 1992). The sampled points constitute a population that is partitioned into several communities (complexes), each of which is permitted to evolve independently (i.e. search the space in different directions). After a certain number of generations, the communities are mixed and new communities are formed through a process of shuffling. This procedure enhances survivability by a sharing of the information (about the search space) gained independently by each search community. A large number of studies (Duan et al., 1992; Thyer et al., 1999) concluded that in general the global population-evolution based algorithm is more effective than multistart local search procedures, which in turn perform better than pure local search methods for calibration of rainfall-runoff models.

Because our initial focus was on the storm hydrograph, each event has been separately calibrated using only respective during-storm observed discharge values while relying on the model for the definition of the antecedent moisture conditions. For this aim, the model was 'warmed up' for a period of six months prior to each event. This was considered a suitable period based on our experience with the model.

## 4. Results and discussion

### 4.1. Results of the minimal calibration

Initially, the SWAT model was applied to the four river basins listed above using the default parameters developed by AVSWAT. Hourly discharge records and uncalibrated flow simulations for the period May 1993 and 2000 were analyzed using an automatic baseflow separation algorithm (Arnold et al., 1995). Table 1 shows the global results of the analyses.

Table 2
Summary of input parameters and range values selected for the calibration of SWAT model

| | Input parameter | Min | Max |
|---|---|---|---|
| SOL_K | Saturated hydraulic conductivity (mm/h) | −50% | +50% |
| SOL_AWC | Available water capacity of the soil layer (mm/mm) | −50% | +50% |
| CH_N | Manning's 'n' value for the main channel | 0.01 | 0.3 |
| CANMX | Maximum canopy storage (mm) | 0.0 | 25.4 |
| REVAPMN | Threshold depth of water in the shallow aquifer for 'revap' or percolation to the deep aquifer to occur (mm) | 0.0 | 500.0 |
| GWQMN | Threshold depth of water in the shallow aquifer required for return flow to occur (mm) | 0.0 | 100.0 |
| ALPHA_BF | Baseflow alpha factor (days) | 0.001 | 1.0 |
| GW_DELAY | Groundwater delay time (days) | 0.001 | 100.0 |
| GW_REVAP | Groundwater 'revap' coefficient | 0.001 | 1.0 |
| TIMP | Snow pack temperature lag factor | 0.01 | 1.0 |
| SURLAG | Surface runoff lag coefficient | 1.0 | 24.0 |
| SMFMN | Min melt fact or for snow (mm/°C day) | 2.0 | 8.0 |
| SMFMX | Max melt factor for snow (mm/°C day) | 2.0 | 8.0 |
| ESCO | Soil evaporation compensation factor | 0.01 | 1.0 |

Table 3
Characteristics of 24 events selected for Blue river basin, simulated values and discharge statistic with SWAT model

| Events | Start time–end time | Observed peak (CMS) | Volume (mm) | Min-calibrated peak (CMS) | Volume (mm) | E[a] | $R^2$ | Slope | Calibrated peak (CMS) | Volume (mm) | E[a] | $R^2$ | Slope |
|---|---|---|---|---|---|---|---|---|---|---|---|---|---|
| 1 | 4/25/1994 0:00–5/8/1994 23:00 | 224 | 59.1 | 222 | 89.98 | 0.21 | 0.55 | 0.68 | 174 | 63.5 | 0.79 | 0.8 | 1.12 |
| 2 | 11/12/1994 0:00–11/27/1994 23:00 | 215 | 43.8 | 261 | 35.3 | 0.9 | 0.93 | 0.89 | 224 | 44.5 | 0.96 | 0.97 | 1.03 |
| 3 | 12/7/1994 0:00–12/13/1994 23:00 | 142 | 22 | 46.4 | 8.3 | 0.17 | 0.98 | 3.35 | 105 | 21.5 | 0.77 | 0.97 | 1.82 |
| 4 | 3/12/1995 0:00–3/20/1995 23:00 | 148 | 30.2 | 119 | 22.3 | 0.72 | 0.89 | 1.52 | 220 | 38 | 0.66 | 0.91 | 0.68 |
| 5 | 5/6/1995 0:00–5/21/1995 23:00 | 289 | 71.8 | 254 | 82.2 | 0.66 | 0.67 | 0.96 | 355 | 69.5 | 0.91 | 0.91 | 0.97 |
| 6 | 9/17/1995 0:00–9/24/1995 23:00 | 47 | 5.1 | 69.4 | 7.3 | −0.39 | 0.83 | 0.46 | 42.2 | 5.2 | 0.87 | 0.87 | 0.95 |
| 7[b] | 9/26/1996 0:00–10/11/1996 23:00 | 156 | 10.6 | 164 | 16.3 | 0.48 | 0.85 | 0.62 | 150 | 10.3 | 0.99 | 0.99 | 1.0 |
| 8 | 10/19/1996 0:00–11/3/1996 23:00 | 253 | 37.4 | 129 | 29.8 | 0.53 | 0.64 | 1.63 | 269 | 36.7 | 0.96 | 0.96 | 1.0 |
| 9[b] | 11/6/1996 0:00–11/21/1996 23:00 | 483 | 48.4 | 278 | 66.2 | 0.75 | 0.82 | 1.1 | 301 | 45.1 | 0.84 | 0.85 | 1.2 |
| 10 | 11/23/1996 0:00–12/6/1996 23:00 | 230 | 62.3 | 268 | 99.1 | 0.2 | 0.66 | 0.69 | 242 | 69.6 | 0.88 | 0.89 | 0.89 |
| 11 | 2/18/1997 0:00–3/5/1997 23:00 | 194 | 44.9 | 93.1 | 44.2 | −0.78 | 0.17 | −0.74 | 176 | 43.7 | 0.9 | 0.9 | 1.09 |
| 12 | 3/25/1997 0:00–3/30/1997 23:00 | 60 | 6.1 | 110 | 17.8 | −4.55 | 0.78 | 0.4 | 38.1 | 8.1 | 0.15 | 0.29 | 0.74 |
| 13 | 6/9/1997 0:00–6/16/1997 23:00 | 130 | 8.2 | 192 | 23 | −1.71 | 0.69 | 0.42 | 120 | 8.1 | 0.94 | 0.94 | 1.0 |
| 14 | 12/20/1997 0:00–12/28/1997 23:00 | 120 | 22 | 98.1 | 25.1 | −1.4 | 0.01 | −0.065 | 118 | 22.2 | 0.97 | 0.97 | 0.97 |
| 15 | 1/3/1998 0:00–1/14/1998 23:00 | 176 | 59.3 | 176 | 64.1 | 0.8 | 0.8 | 1.0 | 188 | 58.9 | 0.94 | 0.94 | 1.02 |
| 16 | 3/6/1998 0:00–3/13/1998 23:00 | 118 | 15.8 | 48 | 31.5 | 0.178 | 0.82 | 0.85 | 129 | 15.9 | 0.98 | 0.98 | 1.01 |
| 17 | 3/14/1998 0:00–3/29/1998 23:00 | 204 | 51.6 | 171 | 64.1 | 0.66 | 0.71 | 1.23 | 213 | 53.9 | 0.90 | 0.9 | 1.01 |
| 18[b] | 1/28/1999 0:00–2/2/1999 23:00 | 25 | 3.6 | 62.6 | 11.3 | −5.0 | 0.93 | 0.42 | 18.4 | 3.8 | 0.72 | 0.73 | 1.0 |
| 19 | 3/27/1999 0:00–4/7/1999 23:00 | 172 | 17 | 222 | 37.6 | 0.01 | 0.83 | 0.61 | 178 | 17 | 0.97 | 0.97 | 1.0 |
| 20 | 6/22/1999 0:00–7/6/1999 23:00 | 29 | 5.7 | 151 | 34.7 | −102.3 | 0.01 | −0.01 | 8.1 | 5.8 | 0.21 | 0.24 | 1.66 |
| 21 | 9/8/1999 0:00–9/24/1999 23:00 | 17 | 3.4 | 35.6 | 8.6 | −7.1 | 0.45 | 0.22 | 13.9 | 2.8 | 0.82 | 0.87 | 0.86 |
| 22 | 12/9/1999 0:00–12/19/1999 23:00 | 26 | 3.0 | 32.4 | 4.7 | −1.19 | 0.71 | 0.39 | 25.6 | 2.5 | 0.95 | 0.97 | 0.92 |
| 23 | 2/22/2000 0:00–3/2/2000 23:00 | 11 | 2.6 | 48.8 | 14.9 | −53.1 | 0.7 | 0.20 | 9.1 | 2.5 | 0.74 | 0.76 | 1.2 |
| 24 | 4/29/2000 0:00–5/11/2000 23:00 | 23 | 4.8 | 89.9 | 21.3 | −29.3 | 0.09 | 0.06 | 20 | 4.9 | 0.91 | 0.91 | 1.0 |

[a] Simulation efficiency (Nash and Sutcliffe, 1970).
[b] Parameters evaluated using only records at which observed values where available.

Table 1 also reports the global results of the manual calibration described in Section 3. These uncalibrated and minimum-calibrated results were analyzed by Reed et al. (2004). This analysis includes the comparison with observed data (calibration and validation periods) and with the simulation results achieved with other applied models, at a variety of river sections (Smith et al., 2004). We note that the calibrated simulations provided and analyzed by Reed et al. (2004) were actually calibrated at a minimal, manual level.

### 4.2. Additional calibration for the Blue River basin

The SWAT model was re-applied to the 1233 km$^2$ Blue River basin. The Blue River basin is depicted in Fig. 1, with the AVSWAT delineated aggregate sub-watersheds and the HRAP grids superimposed. The original simulation framework was left unchanged, with the exception of the following:

(1) Maximum and minimum daily temperature records from five NOAA National Climatic Data Center climate stations, located as shown in Fig. 1, were introduced into the model simulation. The earlier simulations used SWAT's weather-generated daily temperature records derived from statistical parameters relative to five stations.

Use of the new temperature data sets led to a visible improvement of the simulations. Fig. 2 shows the effectiveness of using the temperature records for an event which occurred between 2/20/1997 and 2/26/1997.

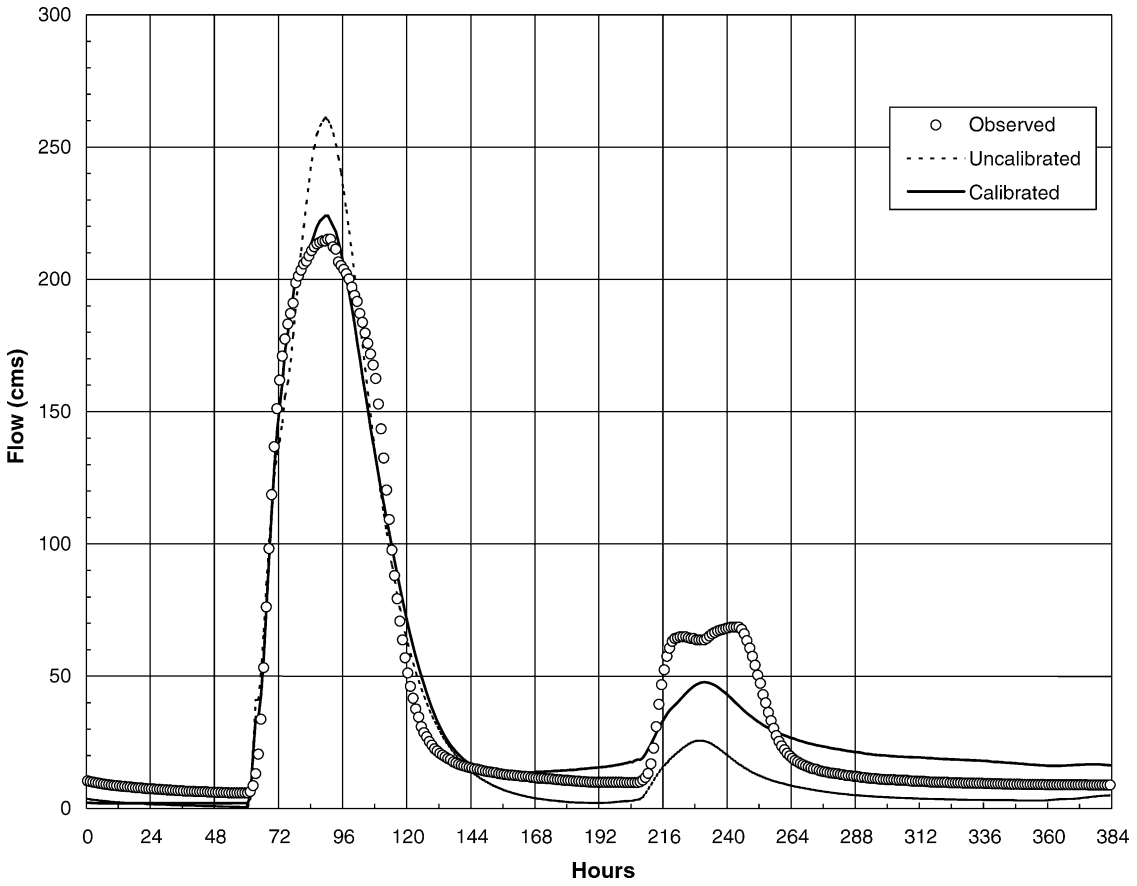


Fig. 3. Simulation of event 2, November 12–27, 1994, Blue River basin. Solid line shows calibrated results; dashed line shows minimal calibration results.

(2) The automatic calibration approach described in Section 3, now implemented in SWAT (Van Griensven, 2002), was applied. The parameters and the respective range values listed in Table 2 have been selected and used within the revised calibration. Parameter values were uniformly adjusted for each HRU by the calibration routines.

Table 3 reports the results of the simulations and the statistical analyses of the selected events before the calibration (minimum calibration) and after the application of the automatic calibration method. Figs. 3–7 show the hydrographs for selected representative events.

### 4.3. Discussion

The results in Table 2 show that the model strategy followed in the manual calibration approach led to a good overall water balance with minimal calibration. This strategy should be considered as a heuristic process based on an initial selection of parameters at the top of their hierarchical water budget sensitivity valid for any watershed. Although the search of the optimal combination of the selected parameters was manually performed, in the future this step could be done automatically, making the entire approach completely objective.

While the focus of our work is to accurately simulate storm events, Reed et al. (2004) showed that

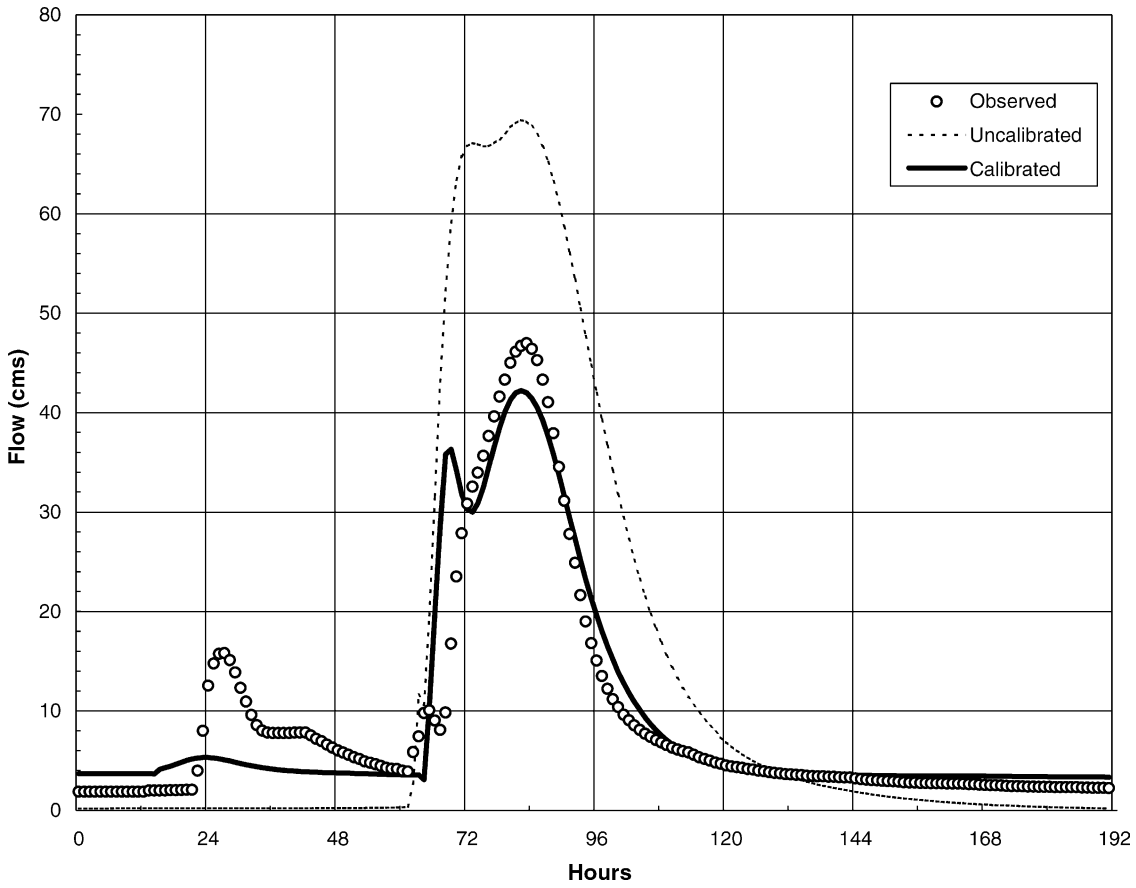


Fig. 4. Simulation of event 6, September 17–24, 1995, Blue River basin. Solid line shows calibrated results; dashed line shows minimal calibration results.

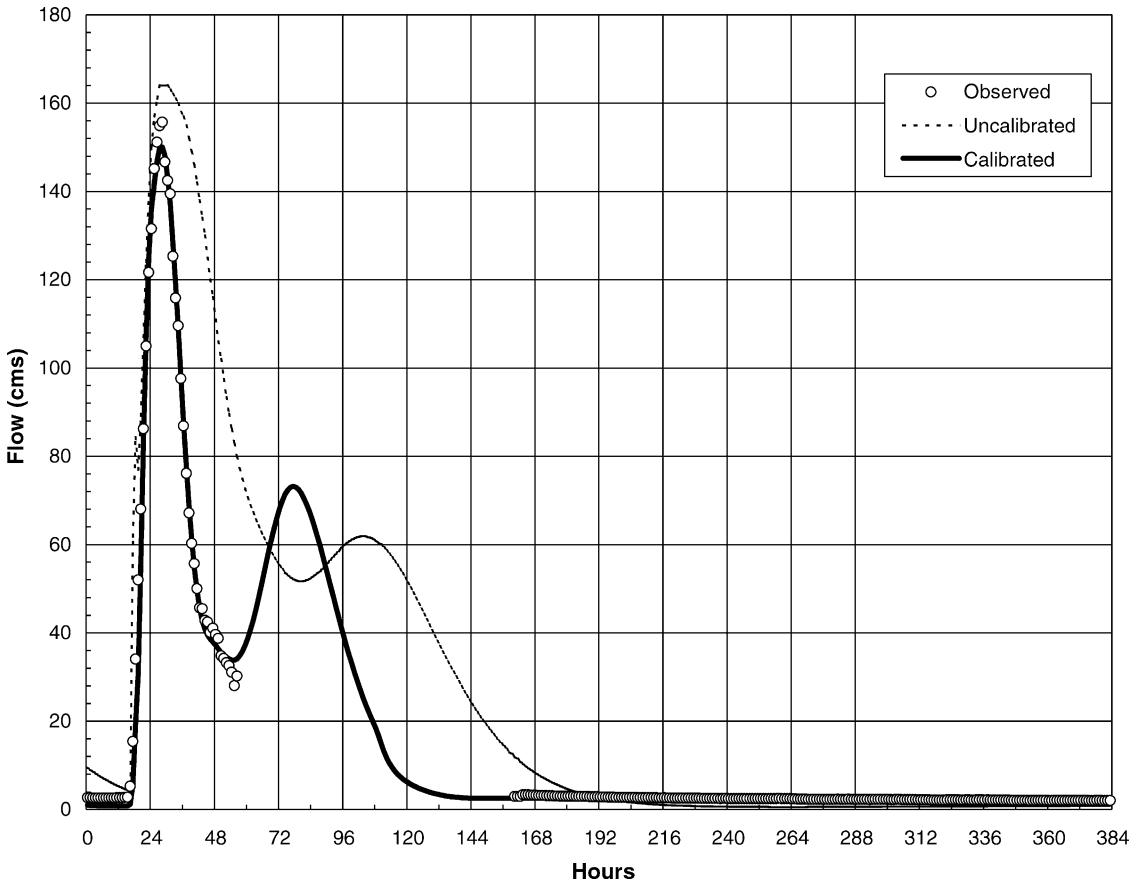


Fig. 5. Simulation of event 7, September 26–October 11, 1996, Blue River basin. Solid line shows calibrated results; dashed line shows minimal calibration results.

our simulations for a number of events were unsatisfactory. However in the present work (see Table 3), most medium and high runoff events (i.e. event 2 shown in Fig. 3, events 9 and 15 shown in Fig. 7, events 4, 5 and 7 shown in Fig. 5, events 8 and 17 shown in Fig. 6) are quite well simulated. For these events, except event 2, the model underestimates the peak flow while favorably estimating the runoff volume. The results also show the general difficulty of the model in simulating small events (events 19–24, events 12–14 and event 6 shown in Fig. 4). For these events, except event 14, it appears that the model considerably overestimates the peak flow.

The results also show that the automatic calibration method (along with the introduction of the daily temperature records) provided a noticeable improvement of the simulation results for the selected events. The simulation efficiency, except events 12 and 20, is over 0.72, with several values over 0.8 and 0.9. In particular, with no exceptions, the approach appears effective in estimating the overall volume of runoff for each event, while adjustment of the resulting peak flows were not always improvements (events 1, 5, 15 and 24). Most probably this is a bias due to the chosen objective function.

Calibration results are particularly positive if we consider that: (1) durations of the selected events are all greater than a week, with the inclusion of components of the hydrograph variously distributed; (2) the automatic calibration method did not include a strategy for distinguishing these components and eventually correlating them to subsets of the input parameters (dominant hydrologic processes); (3) the calibration approach did not

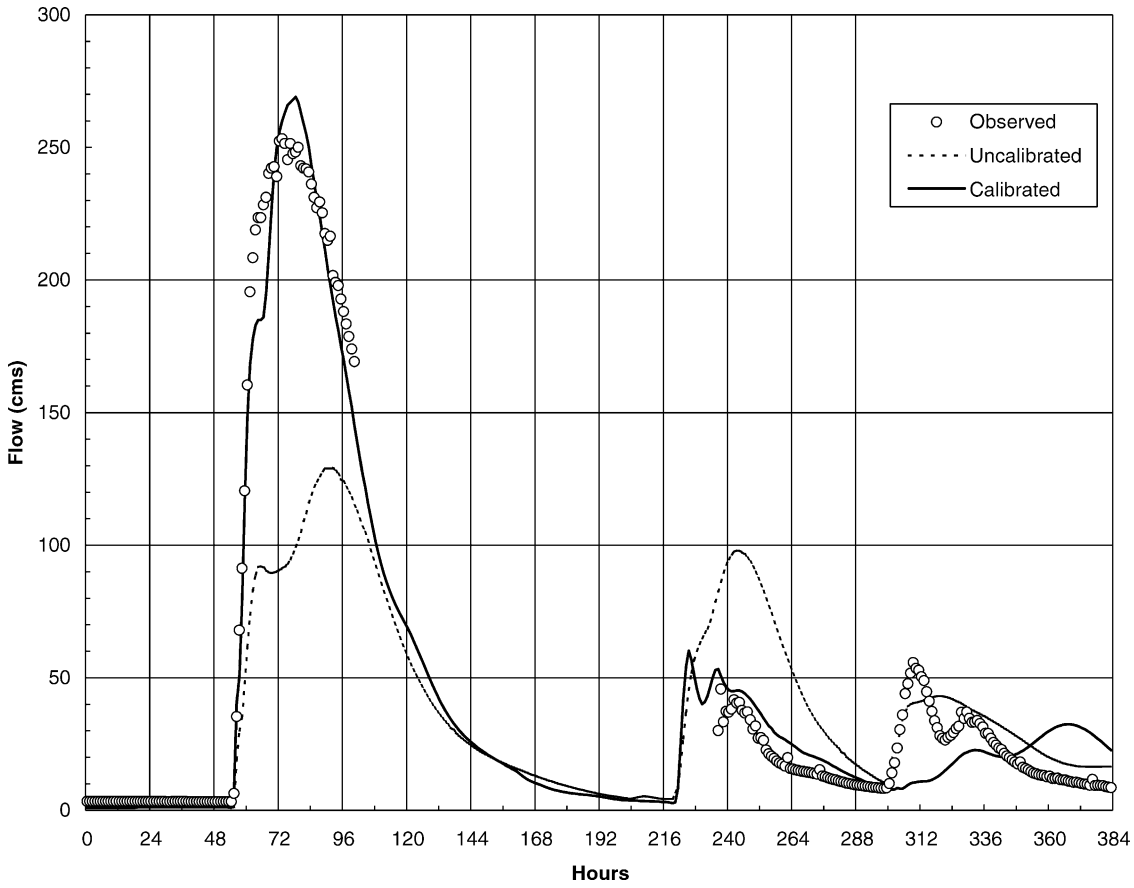


Fig. 6. Simulation of event 8, October 19–November 3, 1996, Blue River basin. Solid line shows calibrated results; dashed line shows minimal calibration results.

include any consideration of errors in the data and parameters as well as their spatial distribution and correlation; (4) the automatic component of the overall calibration with single criteria (vs. multi-criteria) has been applied; and (5) the calibration was performed using streamflow data relative to a single (vs. multiple) stream section.

These are all aspects we intend to investigate in the future along with their verification using the entire observation set on this and other watersheds along with their implication for water quality assessments.

## 5. Concluding remarks

There was the need to establish an initial calibration approach for the SWAT model and its simulations on an hourly basis. In this study the SWAT model was applied with minimal manual calibration in the DMIP project for the entire set of case study watersheds and monitored stream sections, using, for the first time, Stage III radar hourly rainfall data input from NEXRAD. Simulations were fully compared with the respective hourly discharge data and other model simulations by Reed et al. (2004).

A further effort of calibration led to the formulation of a hybrid approach for the SWAT model. The approach is objective in the sense that it establishes explicit steps by which the actual sequence of parameter adjustments is made. The approach adds an automatic component to the manual. Both components involve a prior selection and knowledge about parameters

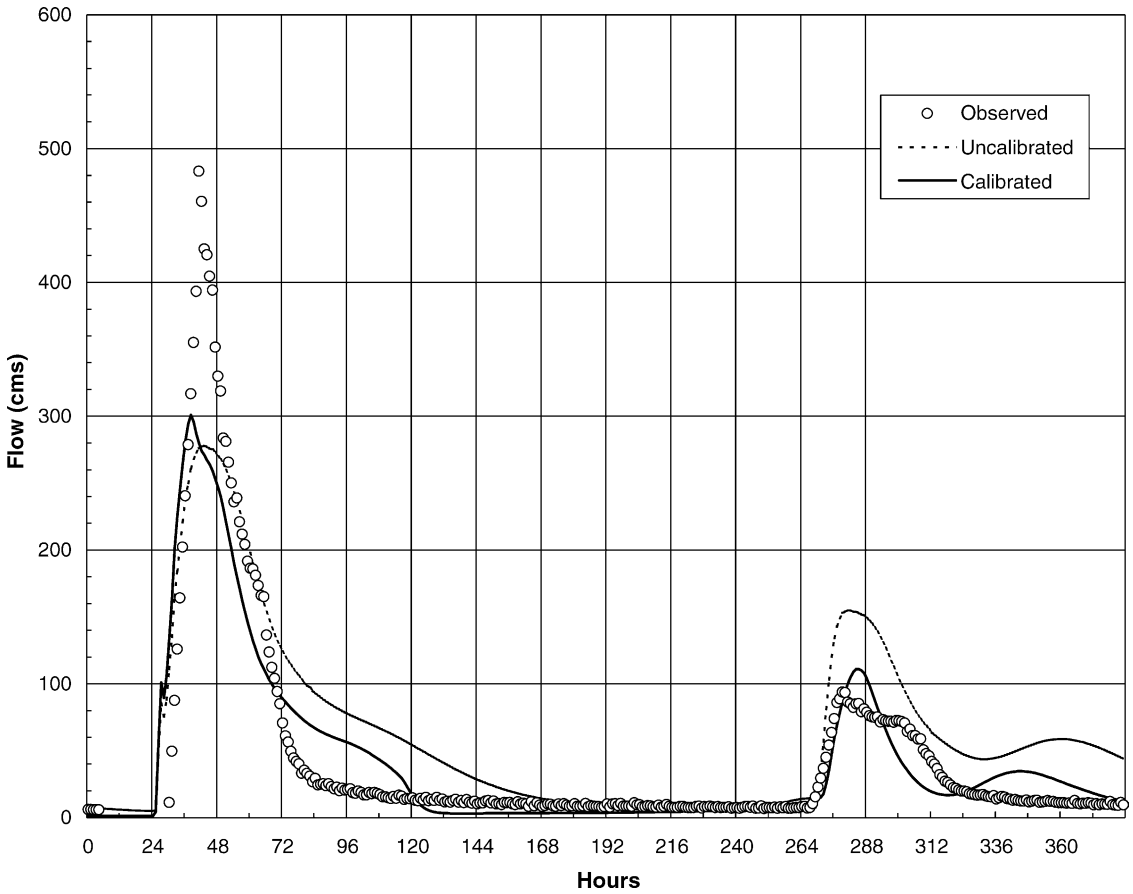


Fig. 7. Simulation of event 9, November 6–21, 1996, Blue River basin. Solid line shows calibrated results; dashed line shows minimal calibration results.

(i.e. specification of realistic limits based on the physical properties).

The results, obtained by using the automatic calibration (SCE) algorithm on a representative set of storm events in the Blue River basin, show significant visual and statistical improvement. In particular, the model was able to effectively reproduce the volumes of water runoff for storm events with a variety of sizes and duration. The results presented here using NEXRAD data are encouraging since several routines have recently been added to SWAT including sub-daily runoff and routing along with the automatic calibration.

In addition, a number of other aspects need to be investigated: the use of multiobjective criteria, methods distinguishing the effect of dominant hydrologic processes, and the use of multiple observation sites. These further investigations and a new program of comparison from the DMIP project should provide direction for improvements of the SWAT model. We consider the DMIP project as a starting point for further development and implications of NEXRAD data for NPS model improvements.

## Acknowledgements

We acknowledge Ann Van Griensven, at the University of California, Riverside, for introducing the SCE-UA algorithm in the SWAT framework.

## References


Arnold, J.G., Allen, P.M., Bernhardt, G., 1993. A comprehensive surface groundwater flow model. Journal of Hydrology 142, 47–69.

Arnold, J.G., Allen, P.M., Muttiah, R.S., Bernhardt, G., 1995. Automated base flow separation and recession analysis techniques. Groundwater 33(6), 1010–1018.

Arnold, J.G., Srinivasan, R., Muttiah, R.S., Williams, J.R., 1998. Large area hydrologic modeling and assessment. Part I. Model development. Journal of American Water Resources Association 34(1), 73–89.

Arnold, J.G., Srinivasan, R., Muttiah, R.S., Allen, P.M., Walker, C., 1999. Continental scale simulation of the hydrologic balance. Journal of American Water Resources Association 35(5), 1037–1052.

Arnold, J.G., King, K.W., Srinivasan, R., Di Luzio, M., 2002. SWAT2000: current capabilities and research opportunities in applied watershed modeling, 2002 ASAE Annual International Meeting, Chicago, IL, July 28–31, 2002, Paper No. 022137.

Baumer, O., Kenyon, P., Bettis, J., 1994. MUUF v2.14 User's Manual, Natural Resource Conservation Service, National Soil Survey Center, Lincoln, Nebraska.

Bouwer, H., 1966. Rapid field measurement of air entry value and hydraulic conductivity of soil as significant parameters in flow system analysis. Water Resources Research 2(4), 729–738.

Boyle, D.P., Gupta, H.V., Sorooshian, S., 2000. Toward improved calibration of hydrologic models: combining the strength of manual and automatic methods. Water Resources Research 36(12), 3663–3674.

Cunge, J.A., 1969. On the subject of a flood propagation method (Muskingum method). Journal of Hydraulic Research 7(2), 205–230.

Di Luzio, M., Srinivasan, R., Arnold, J.G., 2004. A GIS-hydrological model system for the watershed control of agricultural nonpoint and point sources of pollution. Transactions in GIS 8(1), 113–136.

Duan, Q., 1991. A global optimization strategy for efficient and effective calibration of hydrological models. PhD Thesis. Department of Hydrology and Water Resources, University of Arizona, Tucson.

Duan, Q., Sorooshian, S., Gupta, V.K., 1992. Effective and efficient global optimization for conceptual rainfall-runoff models. Water Resources Research. 28(4), 1015–1031.

ESRI (Environmental System Research Institute), 1996a. What's New in ArcView GIS 3.0, ESRI, Redlands, CA.

ESRI (Environmental System Research Institute), 1996b. Using AVENUE, ESRI, Redlands, CA.

Fulton, R.A., Breidenbach, J.P., Seo, D.J., Miller, D.A., 1998. WSR-88D rainfall algorithm. Weather Forecasting 13, 377–395.

Green, W.H., Ampt, G.A., 1911. Studies on soil physics. Journal of Agricultural Science 4(1), 1–24.

Gupta, H.V., Sorooshian, S., Yapo, P.O., 1998. Toward improved calibration of hydrological models: multiple and noncommensurable measures of information. Water Resources Research 34(4), 751–763.

King, K.W., Arnold, J.G., Bingner, R.L., 1999. Comparison of Green-Ampt and curve number methods on Goodwin creek watershed using SWAT. Transactions of the ASAE 42(4), 919–925.

Kuczera, G., 1983. Improved parameter inference in catchment models. 2. Combining different kinds of hydrologic data and testing their compatibility. Water Resources Research 19(5), 1163–1172.

Lindström, G., 1997. A simple automatic calibration routine for the HBV model. Nordic Hydrology 28(3), 153–168.

Madsen, H., Wilson, G., Ammentorp, H.C., 2002. Comparison of different automated strategies for calibration of rainfall-runoff models. Journal of Hydrology 261, 48–59.

Mein, R.G., Larson, C.L., 1973. Modeling infiltration during a steady rain. Water Resources Research 9(2), 384–394.

Nash, J.E., Sutcliffe, J.V., 1970. River flow forecasting through conceptual models. Part 1. A discussion of principles. Journal of Hydrology 10, 282–290.

Nearing, M.A., Liu, B.Y., Risse, L.M., Zhang, X., 1996. Curve numbers and Green-Ampt effective hydraulic conductivities. Water Resources Bulletin 32(1), 125–136.

Pilgrim, D.H., Cordery, I., 1992. Flood routing. In: Maidment, D.R., (Ed.), Handbook of Hydrology, McGraw-Hill, New York, pp. 923–936.

Reed, S., Maidment, D., 1999. Coordinate transformations for using NEXRAD data in GIS-based hydrologic modeling. Journal of Hydrologic Engineering 4(2), 174–182.

Reed, S., Koren, V.I., Smith, M.B., Zhang, Z., Moreda, F., Seo, D.J., DMIP Participants, 2004. Overall distributed model intercomparison project results. Journal of Hydrology DMIP (Special issue).

Smith, M.B., Seo, D.-J., Koren, V.I., Reed, S., Zhang, Z., Duan, Q.-Y., Moreda, F., Cong, S., 2004. The distributed model intercomparison project (DMIP): motivation and experiment design. Journal of Hydrology DMIP (Special issue).

Sorooshian, S., Dracup, J.A., 1980. Stochastic parameter estimation procedures for hydrologic rainfall-runoff models: correlated and heteroscedastic error cases. Water Resources Research 16(2), 430–442.

Sorooshian, S., Duan, Q., Gupta, V.K., 1993. Calibration of rainfall-runoff models: application of global optimization to the Sacramento soil moisture accounting model. Water Resources Research 29, 1185–1194.

Thyer, M., Kuczera, G., Bates, B.C., 1999. Probabilistic optimization for conceptual rainfall-runoff models: a comparison of the shuffled complex evolution and simulated annealing algorithms. Water Resources Research 35(3), 767–773.

USDA-NRCS, US Department of Agriculture-Natural Resource Conservation Service, 1992. State Soil Geographic Database (STATSGO) Data Users' Guide. Publication 1492, US Government Printing Office, Washington, DC.

USGS, US Geological Survey, 1993. Digital Elevation Models—Data Users Guide 5, US Geological Survey, Reston, VA, p. 48.

USGS and USEPA, US Geological Survey and US Environmental Protection Agency, 2000. The National Hydrography Dataset: Concepts and Contents, Available at http://nhd.usgs.gov/chapter1/index.html.

Van Griensven, A., 2002. Developments toward integrated water quality modeling for river basins. PhD Dissertation. VUB Hydrologie Nr. 40. Vrije Universiteit Brussels, Faculty of Applied Sciences, Department of Hydrology and Hydraulic Engineering, p. 236.

Vogelmann, J.E., Howard, S.M., Yang, L., Larson, C.R., Wylie, B.K., Van Driel, N., 2001. Completion of the 1990s National Land Cover Dataset for the conterminous United States from Landsat Thematic Mapper data and ancillary data sources. Journal of American Society for Photogrammetry and Remote Sensing 67(6), 650–662.

Yapo, P.O., Gupta, H.V., Sorroshian, S., 1998. Muti-objective global optimization for hydrological models. Journal of Hydrology 204, 83–97.